Enhanced absorption in optically thin solar cells by scattering from embedded dielectric nanoparticles

James R. Nagel[1] and Michael A. Scarpulla[1,2]

[1] *Department of Electrical and Computer Engineering, University of Utah, Salt Lake City, Utah, USA*
[2] *Department of Materials Science and Engineering, University of Utah, Salt Lake City, Utah, USA*
**scarpulla@eng.utah.edu*

Abstract: We present a concept for improving the efficiency of thin-film solar cells via scattering from dielectric particles. The particles are embedded directly within the semiconductor absorber material with sizes on the order of one wavelength. Importantly, this geometry is fully compatible with the use of an anti-reflective coating (ARC) to maximize light capture. The concept is demonstrated through finite-difference time domain (FDTD) simulations of spherical SiO_2 particles embedded within a 1.0 μm layer of crystalline silicon (c-Si) utilizing a 75 nm ARC of Si_3N_4. Several geometries are presented, with gains in absorbed photon flux occurring in the red end of the spectrum where silicon absorption is weak. The total integrated absorption of incident photon flux across the visible AM-1.5 spectrum is on the order of 5-10% greater than the same geometry without any dielectric scatterers.

OCIS codes: (310.6628) Subwavelength structures, nanostructures; (310.6805) Theory and design; (310.1210) Antireflection coatings.

References and links

1. C. Seassal, Y. Park, A. Fave, E. Drouard, E. Fourmond, A. Kaminski, M. Lemiti, X. Letartre, and P. Viktorovitch, "Photonic crystal assisted ultra-thin silicon photovoltaic solar cell," Proc. SPIE **7002**, 700207 (2008).
2. L. Zeng, Y. Yi, C. Hong, J. Liu, N. Feng, X. Duan, L. C. Kimerling, and B. A. Alamariu, "Efficiency enhancement in Si solar cells by textured photonic crystal back reflector," Appl. Phys. Lett. **89**(11), 111111 (2006).
3. H. A. Atwater, and A. Polman, "Plasmonics for improved photovoltaic devices," Nat. Mater. **9**(3), 205–213 (2010).
4. B. P. Rand, P. Peumans, and S. R. Forrest, "Long-range absorption enhancement in organic tandem thin-film solar cells containing silver nanoclusters," J. Appl. Phys. **96**(12), 7519–7526 (2004).
5. P. Matheu, S. H. Lim, D. Derkacs, C. McPheeters, and E. T. Yu, "Metal and dielectric nanoparticle scattering for improved optical absorption in photovoltaic devices," Appl. Phys. Lett. **93**(11), 113108 (2008).
6. Lumerical Solutions, Inc., *http://www.lumerical.com/*.
7. E. D. Palik, *Handbook of Optical Constants of Solids* (Academic Press, 1998)
8. A. Meldrum, L. A. Boatner, and C. W. White, "Nanocomposites formed by ion implantation: recent developments and future opportunities," Nucl. Instrum. Methods Phys. Res. B **178**(1-4), 7–16 (2001).
9. V. V. Voronkov, and R. Falster, "Latent complexes of interstitial boron and oxygen dimers as a reason for degradation of silicon-based solar cells," J. Appl. Phys. **107**(5), 053509 (2010).
10. J. A. Kong, *Electromagnetic Wave Theory* (EMW Publishing, 2000).
11. C. F. Bohren, and D. R. Huffman, *Absorption and Scattering of Light by Small Particles* (John Wiley & Sons, 1983).
12. D. Derkacs, S. H. Lim, P. Matheu, W. Mar, and E. T. Yu, "Improved performance of amorphous silicon solar cells via scattering from surface plasmon polaritons in nearby metallic nanoparticles," Appl. Phys. Lett. **89**(9), 093103 (2006).
13. D. M. Schaadt, B. Feng, and E. T. Yu, "Enhanced semiconductor optical absorption via surface plasmon excitation in metal nanoparticles," Appl. Phys. Lett. **86**(6), 063106 (2005).

#127681 - $15.00 USD Received 28 Apr 2010; revised 17 May 2010; accepted 17 May 2010; published 19 May 2010

1. Introduction

Thin-film silicon solar cell technology is a promising avenue for reducing the bulk material costs of photovoltaic devices. Because of its natural abundance, non-toxicity, and established industry, silicon is a nearly ideal material for GW- and TW-scale energy production. Unfortunately, silicon suffers from long optical absorption lengths at the red and near-infrared wavelengths, thereby requiring thicknesses of a few hundred microns in order to fully utilize the available power in the incident solar spectrum.

Several methods have been recently explored to improve light absorption in optically-thin semiconducting films, typically involving schemes for laterally scattering normally-incident light. This forces the light to propagate through a longer path length for the same given thickness of active material, thereby improving light absorption and photocarrier generation. For example, one method attempts to scatter light directly from the front surface of the cell through the use of an etched diffraction grating [1]. Another example uses a distributed Bragg reflector at the rear of the cell to scatter light from the bottom boundary [2]. Unfortunately, these strategies are often incompatible with thin-film solar cells because the necessary texture dimensions (≈1 μ m) can easily exceed the film thickness.

Plasmonic noble-metal nanoparticles can also be placed on top of the cell to achieve enhanced coupling and lateral scattering [3]. Because of the large scattering cross-sections of such particles, significant efficiency gains have been observed with relatively small particle sizes (25-100 nm) and sparse particle density. However, such strategies can be difficult to practically implement in the presence of an anti-reflective coating (ARC). As is demonstrated herein, simply putting plasmonic nanoparticles on top of a conventional ARC may reduce performance, and one must carefully optimize the ARC and nanoparticle layer as a combined optical system.

In this work, we propose a distinct mechanism of lateral scattering using dielectric particles placed directly within the absorber layer itself. Such dielectric particles are almost perfectly lossless and have broad regions of high scattering cross section, thus making them ideal for use with the solar spectrum. Although their scattering cross sections are lower than those of plasmonic particles on resonance, the absence of absorption results in comparable light absorption enhancements in the absorber layer. Similar ideas have been explored in work such as [4], wherein silver nanoclusters were embedded within thin-film organic solar cells as a mechanism for light scattering. Another recent work has demonstrated increased light absorption using dielectric nanoparticles on top of the absorber layer [5]. The main difference in this work is our combination of the two concepts and then integration with an ARC. Several geometries are presented as demonstrations of the dielectric-scattering concept, with typical power absorption gains on the order of 5-10% relative to unmodified Si layers. We focus on the optical effects of these dielectric scattering centers and discuss only briefly some possible routes for physical realization.

2. Solar cell model

The baseline model for a thin-film solar cell is depicted by the inset in Fig. 1(a). The model was simulated with the Lumerical FDTD Solutions software [6] and dielectric functions from sampled data in [7]. For simplicity, we limited the model to 1.0 μm of c-Si covered by a layer of Si_3N_4 serving as the ARC. The thickness of the ARC was set to 75 nm to maximize light transmission into the c-Si layer around a wavelength of λ = 600 nm, which is the approximate peak of the AM-1.5 solar spectrum. Although a real solar cell would also be doped to form a p-n junction, the dielectric function of Si is not significantly altered in the spectral range below 1200 nm for reasonable doping concentrations, and so need not be accounted for in this model. Unless noted otherwise, periodic boundary conditions (PBCs) were used at the lateral (x-y) boundaries of the simulation volume to mimic the effects of an infinite periodic array, thereby including any coupling effects between neighboring nanoparticles. The top and

#127681 - $15.00 USD Received 28 Apr 2010; revised 17 May 2010; accepted 17 May 2010; published 19 May 2010

bottom boundaries of the simulation were perfectly matched layers (PMLs), thus simulating semi-infinite extent in both the air and Si. This makes our findings more general and geometry- independent than, for example, if we had used a reflecting metal layer at the back surface.

We chose to use SiO_2 in Si to demonstrate this concept primarily because SiO_2 (n ≈1.5) has good dielectric constant contrast with Si (n ≈3.6), and is almost perfectly lossless in the visible spectrum. Also, under the right circumstances Si/SiO_2 interfaces may have extremely low dangling bond densities and interface recombination velocities. SiO_2 nanoparticle arrays are potentially realizable in c-Si via ion-implantation and annealing methods similar to those used to form some silicon-on-insulator wafers [8]. However, the nucleation and growth of SiO_2 nanoparticles from solutions of O in Si, as commonly used with internal gettering schemes, in many cases results in incoherent Si/SiO_2 interfaces with high recombination velocities [9]. Alternatively, SiO_2 or similar nanoparticles could be prepared on a Si surface and then overgrown with c-Si or amorphous Si (a-Si) deposited by a variety of thin-film growth methods. The hydrogenation and fluorination used to passivate a-Si would also tend to passivate dangling bonds at the SiO_2 interfaces. The use in a-Si cells may therefore be even more advantageous than in c-Si.

To quantify the effects of dielectric scattering by embedded spheres, we first calculated the absorption factor $A(z,\lambda)$, defined as the fraction of incident power density that gets absorbed within a given z-depth of the c-Si layer. If we then define $T(z,\lambda)$ as the power transmission coefficient through an xy-plane at depth z, the absorption factor may be expressed as

$$A(z,\lambda) = T(0,\lambda) - T(z,\lambda), \tag{1}$$

where $T(z,\lambda)$ indicates the total fraction of incident power that enters the c-Si layer. In other words, the absorption factor is simply the difference between power that physically enters the cell at the surface and power that exits through a plane at some given depth. From this notation, we may further define the flux absorbance $S(z,\lambda)$ by the expression

$$S(z,\lambda) = A(z,\lambda)\Phi_o(\lambda), \tag{2}$$

where $\Phi_0(\lambda)$ is the AM-1.5 spectrum in units of photon flux density (photons / s^{-1} nm^{-1} m^{-2}). The quantity $S(z,\lambda)$ therefore represents the spectral flux density of photons that are captured within a given thickness of active semiconductor material. If we further assume perfect internal quantum efficiency, then the total integrated flux absorbance across the visible spectrum is directly proportional to short-circuit current density.

The plot in Fig. 1(a) shows two absorption spectra of interest for the baseline solar cell. These values were computed using FDTD simulation and then validated by analytical multi-layer calculations [10]. The top curve represents $S(\infty,\lambda)$, which signifies the total photon flux that physically enters the c-Si layer from the surface. Thus, if the c-Si layer were infinitely thick, then all of these photons would eventually be absorbed by the semiconductor, and $S(\infty,\lambda)$ signifies the upper-bound of potentially available photons. The bottom curve represents $S(1\mu m,\lambda)$ and signifies the photons that are captured within the 1.0 μm layer of c-Si. Ideally, $S(1\mu m,\lambda)$ should approach $S(\infty,\lambda)$ as closely as possible, since this would imply that all light entering the c-Si is absorbed within the top 1.0 μm layer. In the spectral region below $\lambda = 450$ nm, the absorption length of c-Si is very short and the two curves naturally overlap. Towards the red end of the spectrum, the long absorption lengths manifest as a divergence between $S(\infty,\lambda)$ and $S(1\mu m,\lambda)$, thus causing the curves to gradually split apart. The area between these two curves represents un-captured photons by the top 1.0 μm layer,

#127681 - $15.00 USD Received 28 Apr 2010; revised 17 May 2010; accepted 17 May 2010; published 19 May 2010

and any changes that increase the total area under the $S(1\mu m,\lambda)$ curve represent an improvement in the solar cell design.

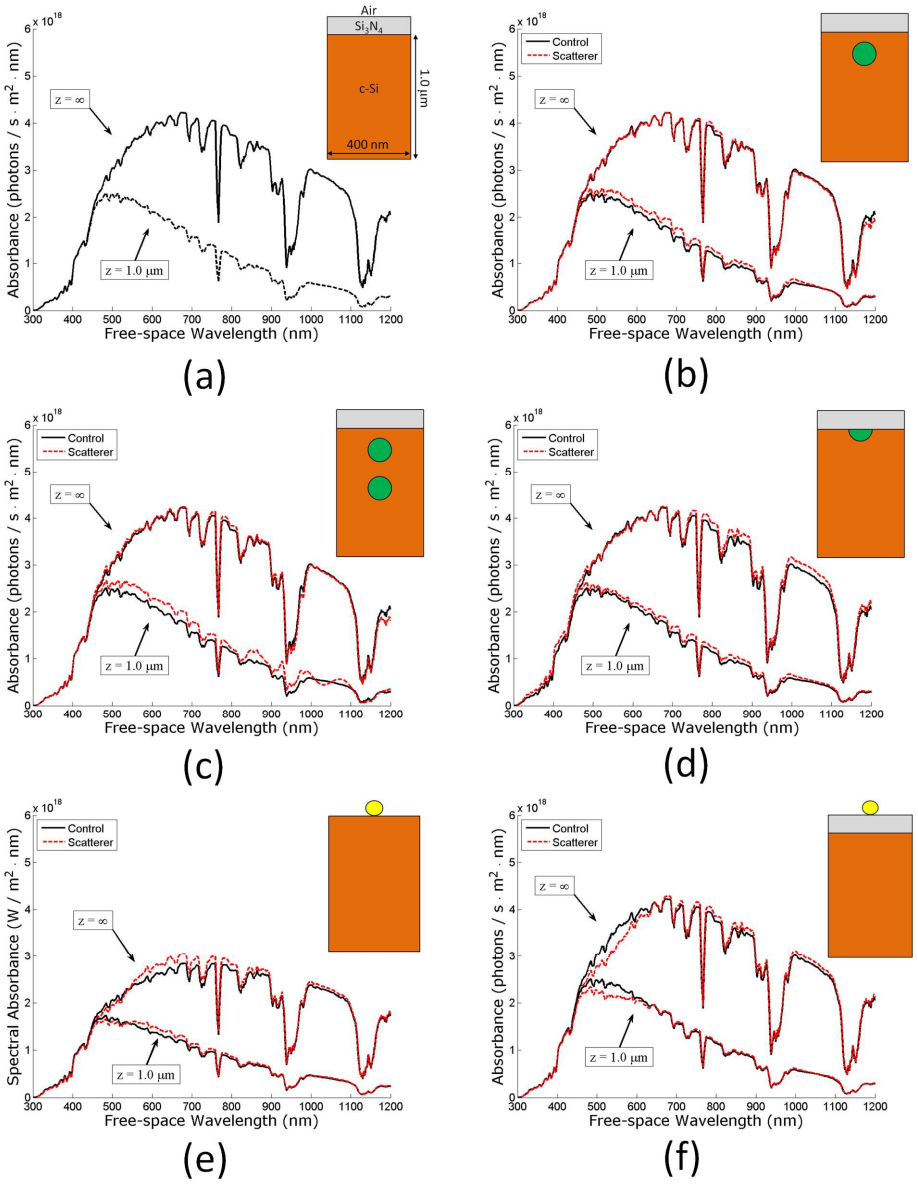

Fig. 1. Simulated photon absorbencies of the thin-film silicon cell with an ARC. Figure (a) summarizes the baseline solar cell with no dielectric scatterer; (b) 6.3% gain using a single SiO_2 sphere with diameter D = 100 nm centered at a depth of z = 150 nm; (c) 12.4% gain using a second sphere placed at a depth of z = 650 nm; (d) 7.4% gain using a hemisphere placed at the c-Si surface; (e) 2.2% gain using an Au sphere placed atop the c-Si with no ARC, but still 26.9% less than part (a); (f) 2.1% loss using an Au sphere (D = 100 nm) placed atop the ARC.

3. Simulation results

We first examine the scattering cross sections of spherical SiO_2 nanoparticles embedded in an infinite c-Si medium. Classical Mie theory [11] gives the scattering efficiency Q_{scat} (≡

#127681 - $15.00 USD Received 28 Apr 2010; revised 17 May 2010; accepted 17 May 2010; published 19 May 2010

scattering cross-section/geometric area) for different diameter spheres, as plotted in Fig. 2. Because the imaginary component of the Si dielectric function is so small compared to the real component in the visible, it may be ignored to first order. As can be seen, the scattering efficiency for SiO_2 spheres remains relatively high ($Q_{scat} \approx 2$) over broad regions of free-space wavelength, but gradually tapers off as wavelength increases. Smaller diameter spheres also tend to lose their scattering efficiencies at shorter wavelengths while larger spheres have large volume that could otherwise be filled with semiconductor to collect photons. We therefore chose 200 nm for the diameter for the spheres as a reasonable balance between broadband scattering and physical size for this particular slab thickness of 1 μm. However, larger diameter SiO_2 spheres (e.g. ≥300 nm in Fig. 2) maintain $Q_{scat} \approx 2$ out to the near-infrared (NIR) where the Si absorption coefficient becomes very small. Thus the use of larger nanoparticles coupled with Si films a few μm thick can even further improve the red-NIR performance while still maintaining low Si material usage. Additionally, greater scattering efficiency may also be achieved through the use of materials with a stronger dielectric contrast against c-Si although interface recombination may preclude the use of arbitrary materials in practice. We are currently investigating these and other related implementations of this concept.

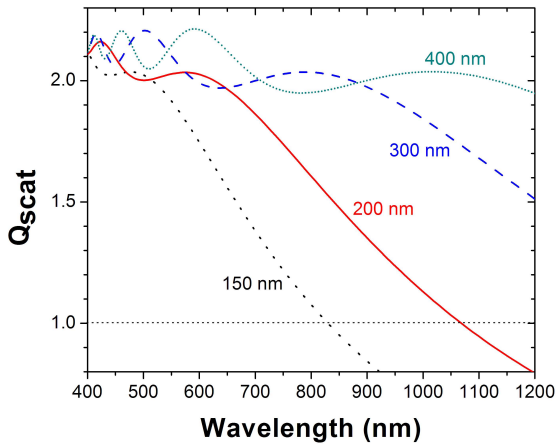

Fig. 2. Mie scattering efficiency of SiO2 spheres of diameters D indicated embedded in an infinite medium of c-Si.

To demonstrate the effectiveness of sub-surface scattering from embedded dielectric nanoparticles, consider the model in Fig. 1(b) of a SiO_2 sphere with diameter D = 200 nm centered at a depth of z = 150 nm beneath the c-Si/Si_3N_4 interface. The xy-span of the simulation was 400 nm × 400 nm, which translates into a geometric area coverage of 19.6% in the x-y plane. This is the same coverage reported in [12] for producing the maximum plasmon enhancement from 100 nm-diameter Au spheres. The dielectric sphere was sampled at a uniform grid resolution of 1.0 nm, with a non-uniform mesh automatically generated for the rest of the simulation domain. The simulation results for this geometry are plotted in Fig. 1(b) and then compared to the baseline cell.

The first thing to note is how $S(\infty,\lambda)$ is relatively unperturbed, thereby demonstrating that the absorption enhancement concept results from lateral scattering within the cell as opposed to suppression of external reflection. A few regions of the spectrum do exhibit a slight, measurable decline, which is expected by perturbing the conditions for which the ARC was optimized. This is due to trace amounts of back-scattered energy from the dielectric particles that escape back into the air. Nevertheless, we also see that $S(1\mu m,\lambda)$ has been

#127681 - $15.00 USD Received 28 Apr 2010; revised 17 May 2010; accepted 17 May 2010; published 19 May 2010

improved across nearly the entire spectrum above 450 nm, resulting in 6.3% greater absorption over the baseline case with an ARC without any embedded nanoparticles.

Further insight into this efficiency gain may be realized by simulating a single particle in isolation and examining the electric field profiles like Fig. 3(a) (Media 1). This was accomplished by using absorbing boundary conditions instead of periodic for all edges of the simulation. In the absence of any particles, the field profile would simply follow an exponential decay along the z-direction as the fields are gradually absorbed by the semiconductor. When the particle is introduced, edge diffraction forces power into off-normal angles as seen by the chevrons of high field intensity. When periodic boundaries are introduced, the result is a field profile like that in Fig. 3(b) (Media 2). In this case, the scattered fields superimpose on each other and manifest as regions of constructive and destructive interference. In particular, the intense antinodes near z = 550 nm are indicative of a strong convergence of multiple scattered waves. It is therefore natural to suppose that a second layer of particles placed near this depth should boost the overall efficiency by scattering even more power into lateral modes. To test this hypothesis, we placed a second sphere at a depth of z = 650 nm as depicted in Fig. 1(c). As the results show, the spectral absorbance was further increased over nearly the entire visible spectrum, and the total integrated photon gain nearly doubled to 12.4% for the same projected area coverage.

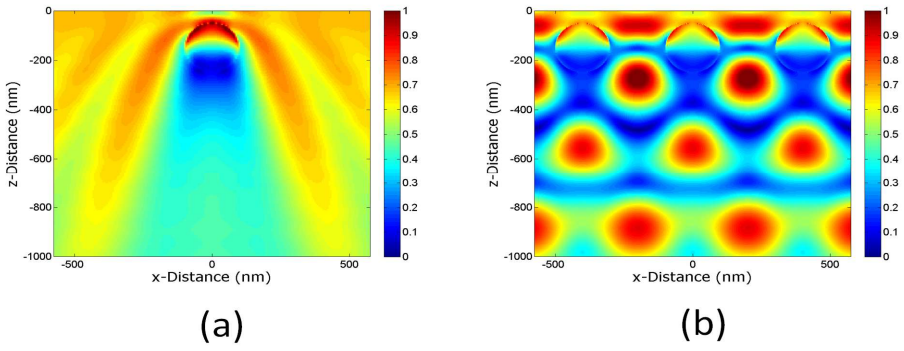

Fig. 3. Peak electric field intensity profile (arbitrary units) at a wavelength of λ = 700 nm for (a) single particle in isolation (Media 1) and (b) periodic array of particles (Media 2). Similar results may be seen across the entire spectrum. Time-domain animations of these images are available in the supporting online material.

Another geometry of interest is depicted in Fig. 1(d), which places a SiO_2 hemisphere directly at the surface of the c-Si layer. Such a geometry could be produced via oxidation of selected areas through well-established Si-processing techniques for obtaining interfaces with low recombination velocity. The absorption gain in this case was found to be 7.4%, with much of the improvement falling below λ = 500 nm. Though similar in principle to surface texturing, the feature size is here is sub-wavelength. Note that this modification of the ARC/Si interface results in both more power entering the cell as well as lateral scattering enhancement.

Given the recent progress in plasmon enhancement of solar cells, it is useful to compare sub-surface dielectric scattering against scattering from surface plasmons on metallic nanoparticles. Because of the large number of design degrees of freedom, only a small subset will be considered herein to illustrate a few key points. These simulation results are summarized in Figs. 1(e) and 1(f). The first case is similar in design to previous work such as [13], which places Au nanospheres (D = 100 nm) directly atop the semiconductor with no ARC. As expected, this geometry succeeds in improving efficiency of the cell by 2.2% over the same geometry without any particles. However, when compared to the baseline cell in Fig. 1(a), the efficiency is still 26.9% less than if the nanoparticles were removed entirely and

#127681 - $15.00 USD Received 28 Apr 2010; revised 17 May 2010; accepted 17 May 2010; published 19 May 2010

replaced by an ARC. Thus it should be realized that a conventional ARC may be more effective than unoptimized nanoparticle scattering schemes at increasing the power coupled into a solar cell.

The second case shows the same nanoparticle geometry after inserting the ARC between the c-Si and the Au nanospheres. Clearly, the Au spheres are now a net detriment to the cell, resulting in 2.1% fewer photons being absorbed at normal incidence. This is because metal particles disrupt the phase-matching properties of the ARC, thereby leading to fewer photons entering the absorber layer. Although we have yet to consider off-normal incidence, it appears very likely that the most advantageous solar cell geometries for enhancing light absorption should always include, and be compatible with, a simple ARC.

4. Grating and coupling effects

As stated previously, using periodic boundary conditions is equivalent to simulation of an infinite array of particles. The next obvious questions are how much of the efficiency improvement can be ascribed to the array structure, how much is caused by individual particle scattering, and how coupling interactions between adjacent particles affect performance. These questions begin to be answered in Fig. 4, which shows efficiency gain as a function of particle density. At sparse densities (< 10^8 particles/cm^2), the inter-particle spacing is much greater than the wavelength in Si and well-outside the scattering cross-section. Thus, each nanoparticle is effectively an isolated scatterer like that in Fig. 2(a). Under such ideal conditions, the scattering enhancement of each new particle adds a linear contribution to the net photon absorption within the cell, as is evidenced by the nearly linear slope below 10^8 cm^{-2}. The diminishing return in cell efficiency enhancement can be understood by the overlap of scattering cross sections, which effectively reduces the power scattered laterally by each nanoparticle. Similar physics is at play in the peaking of the efficiency enhancement of metallic nanoparticle arrays. However, the scattering cross sections are larger for metallic arrays on resonance, and so the effects peak at lower areal density.

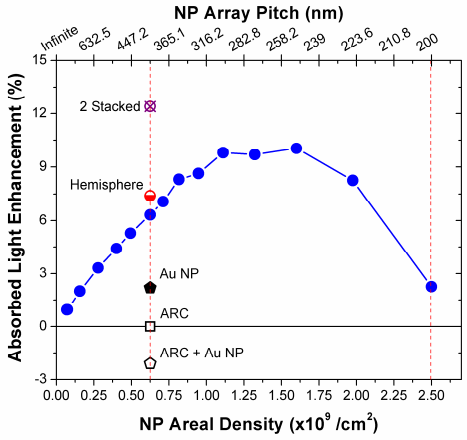

Fig. 4. Efficiency trends versus particle density for periodic arrays of D = 200 nm diameter spheres of SiO_2 embedded in c-Si at a depth of 150 nm. The points along the red vertical line at 6.25 x 10^8 / cm^2 (400 nm spacing) summarize the absorption changes for the geometries in Fig. 1. At 2.5 x 10^9 / cm^2 (200 nm), the dielectric spheres touch.

5. Discussion and conclusions

This work introduces an approach for enhancing the light absorption in thin-film solar cells by placing dielectric nanoparticles within the absorber layer itself. This approach allows the large efficiency gains from a traditional ARC to be coupled with the long-wavelength enhancement

#127681 - $15.00 USD Received 28 Apr 2010; revised 17 May 2010; accepted 17 May 2010; published 19 May 2010

from lateral scattering by nanoparticles. This concept is compatible with the use of arbitrarily-optimized anti-reflective coatings (i.e. single or multiple-layer designs), surface texturing, and various other light-trapping schemes.

Although we have considered the specific case of spherical SiO_2 nanoparticles in Si, the finding of enhanced light absorption will hold generally for any combination of materials with contrasting dielectric constants. The key requirements when choosing a material for the embedded dielectric particles are 1) that the particles be electrically and optically lossless, 2) that the particles have a strong scattering efficiency in the forward/lateral directions, and 3) for solar cell applications, that the dielectric and absorbing medium form low-recombination interfaces. Generally, this approach is most useful for indirect bandgap materials such as Si and Ge. However it could be advantageously applied in a-Si because of its lower absorption efficiency. It could also be used in optically thin layers of organic or inorganic absorbers. We hope that this concept can be advantageously used experimentally to enhance solar cells in some of the implementations we have discussed as well as others we have not.

Acknowledgments

We gratefully thank Dr. Steve Blair for access to the computational resources used in this work.

#127681 - $15.00 USD Received 28 Apr 2010; revised 17 May 2010; accepted 17 May 2010; published 19 May 2010